A Comparison of ^{18}F-DCFPyL, ^{18}F-NaF, and ^{18}F-FDG PET/CT in a Prospective Cohort of Men with Metastatic Prostate Cancer

Aloÿse Fourquet[1], Adrian Rosenberg[1], Esther Mena[1], Joanna J. Shih[2], Baris Turkbey[1], Maxime Blain[3], Ethan Bergvall[1], Frank Lin[1], Stephen Adler[4], Ilhan Lim[5], Ravi A. Madan[6], Fatima Karzai[6], James L. Gulley[6], William L. Dahut[6], Bradford J. Wood[3], Richard Chang[3], Elliot Levy[3], Peter L. Choyke[1], and Liza Lindenberg[1,7]

[1]*Molecular Imaging Branch, National Cancer Institute, National Institutes of Health, Bethesda, Maryland;* [2]*Division of Cancer treatment and Diagnosis: Biometric Research Program, National Cancer Institute, National Institutes of Health, Bethesda, Maryland;* [3]*Center for Interventional Oncology, Radiology and Imaging Sciences, Clinical Center, National Cancer Institute, National Institutes of Health, Bethesda, Maryland;* [4]*Clinical Research Directorate, Frederick National Laboratory for Cancer Research, National Cancer Institute, National Institutes of Health, Bethesda, Maryland;* [5]*Department of Nuclear Medicine, Korea Cancer Center Hospital, Korea Institute of Radiological and Medical Sciences, Seoul, Korea;* [6]*Genitourinary Malignancies Branch, National Cancer Institute, National Institutes of Health, Bethesda, Maryland; and* [7]*F. Edward Hebert School of Medicine, Uniformed Services University of the Health Sciences, Bethesda, Maryland*

^{18}F-DCFPyL, ^{18}F-sodium fluoride (^{18}F-NaF), and ^{18}F-FDG PET/CT were compared in a prospective cohort of men with metastatic prostate cancer (PCa). **Methods:** Sixty-seven men (group 1) with documented metastatic PCa underwent ^{18}F-DCFPyL and ^{18}F-NaF PET/CT and a subgroup of 30 men (group 2) underwent additional imaging with ^{18}F-FDG PET/CT. The tracers were compared for their detection rates, imaging concordance, associations with prostate-specific antigen (PSA), treatment at the time of imaging, and castration status. **Results:** Overall, 61 men had metastatic disease detected on one or more scans, and 6 men had no disease uptake on any of the PET/CT scans (and were subsequently excluded from the analysis). In group 1, ^{18}F-NaF detected significantly more metastatic lesions than ^{18}F-DCFPyL (median of 3 lesions vs. 2, P = 0.001) even after eliminating benign causes of ^{18}F-NaF uptake. This difference was particularly clear for men receiving treatment (P = 0.005) or who were castration-resistant (P = 0.014). The median percentage of bone lesions that were concordant on ^{18}F-DCFPyL and ^{18}F-NaF was 50%. In group 2, ^{18}F-DCFPyL detected more lesions than ^{18}F-FDG (median of 5 lesions vs. 2, P = 0.0003), regardless of PSA level, castration status, or treatment. The median percentage of lesions that were concordant on ^{18}F-DCFPyL and ^{18}F-FDG was 22.2%. This percentage was slightly higher for castration-resistant than castration-sensitive men (P = 0.048). **Conclusion:** ^{18}F-DCFPyL PET/CT is the most versatile of the 3 PET agents for metastatic PCa; however, ^{18}F-NaF detects more bone metastases. Imaging reveals substantial tumor heterogeneity with only 50% concordance between ^{18}F-DCFPyL and ^{18}F-NaF and 22% concordance for ^{18}F-DCFPyL and ^{18}F-FDG. These findings indicate considerable phenotypic differences among metastatic lesions.

Key Words: prostate cancer; metastatic; PSMA; NaF; FDG

J Nucl Med 2022; 63:735–741
DOI: 10.2967/jnumed.121.262371

Prostate cancer (PCa) is the second leading cause of cancer death among men in the United States, with a 5-y survival rate of only 31% in men with metastatic disease (*1*). In recent years, precision medicine has offered the hope of improving outcome with treatments tailored to the molecular and clinical characteristics of an individual patient's malignancy (*2,3*).

In this context, several targeted radiotracers have emerged to assess PCa by PET/CT. ^{18}F-sodium fluoride (^{18}F-NaF) demonstrates uptake at sites of bone remodeling and osteoblastic activity, with higher sensitivity and specificity for detecting bone metastases than conventional bone scintigraphy (*4,5*). ^{18}F-DCFPyL targets prostate-specific membrane antigen (PSMA), a membrane glycoprotein highly expressed on PCa cells, especially in metastatic disease (*6–8*). The most widely used PET agent, ^{18}F-FDG, reflects glucose metabolism commonly upregulated in malignant cells. Although most localized PCa tumors are not ^{18}F-FDG–avid (*9*), its uptake increases with aggressive and widely metastatic disease (*10*). Direct comparisons of these agents could cast light on their relative value in men with metastatic PCa.

Therefore, we prospectively compare the performance of ^{18}F-DCFPyL with ^{18}F-NaF and ^{18}F-DCFPyL with ^{18}F-FDG in men with metastatic PCa to understand patterns of overlap and discordance and their potential significance.

MATERIALS AND METHODS

Patient Selection and Study Design

This single-institution open-label prospective, Health Insurance Portability and Accountability Act–compliant study was approved by the institutional review board (NCT03173924) and radiation safety branch. All patients were enrolled after written informed consent was obtained. Eligibility criteria included men with histopathologically confirmed PCa and identifiable metastatic disease on standard-of-care imaging (CT or conventional bone scan). Exclusion criteria included subjects for whom participating would significantly delay standard therapy. There were no exclusion criteria regarding prior or ongoing therapies. Diagnostic and prior treatment history, castration status, and current treatments were recorded after clinical review of medical records.

Received Mar. 30, 2021; revision accepted Aug. 5, 2021.
For correspondence or reprints, contact Liza Lindenberg (liza.lindenberg@nih.gov).
Published online Sep. 2, 2021.

PET Imaging Protocol

Group 1 subjects underwent ^{18}F-DCFPyL and ^{18}F-NaF PET/CT on separate occasions but within 35 d of each other. ^{18}F-DCFPyL was intravenously injected (mean injected dose, 291.3 MBq [range, 221.4–399.7 MBq]), followed by a head-to-toe PET/CT scan at a mean time of 121.7 ± 7.9 min after injection. ^{18}F-NaF was administered intravenously (mean injected dose, 125.2 MBq [range, 97.9–201.7 MBq]), followed by a head-to-toe PET/CT at a mean time of 63.7 ± 6.0 min after injection.

A subcohort of 30 patients imaged with ^{18}F-DCFPyL also underwent ^{18}F-FDG PET/CT imaging on a separate occasion (group 2) within 33 d of each other. ^{18}F-FDG was administered intravenously (mean injected dose, 377.0 MBq [range, 327.3–433.7 MBq]), with whole-body scanning at a mean time of 61.4 ± 4.6 min after injection.

Imaging was performed on a 3D time-of-flight–mode Discovery MI DR camera (GE Healthcare) with low-dose (120 kV, 60 mAs) CT-based attenuation correction along with random, normalization, dead time and scatter correction.

When technically feasible and after patient consent, a biopsy of at least 1 suggestive lesion identified on imaging was performed within 4–6 mo of scanning.

Imaging Analysis

PET/CT review and analysis was performed using a MIM workstation (version 6.9.2; MIM Software Inc.) by 3 experienced nuclear medicine physicians. Only lesions that were highly suggestive of metastatic or recurrent disease by consensus were included. Indeterminate lesions were excluded from the analysis. In particular, benign causes of increased uptake on ^{18}F-NaF scans were eliminated from the dataset.

SUV, tumor volume (TV), and total lesion uptake (TLU) were reported for every lesion after a semiautomatic segmentation analysis tool for contouring (PET-Edge) was applied. TLU was calculated as the multiplication of SUV_{mean} and TV for each lesion. All values obtained per person were summed to calculate the TLU at the patient level. The total tumor burden (TB) was calculated as the sum of TV from all reported lesions per person.

When the scan showed extensive disease, with lesions too numerous to delineate manually, a semiautomatic software algorithm based on an SUV threshold was used. The pathologic threshold SUV was set at 3 for both ^{18}F-DCFPyL and ^{18}F-FDG and 10 for ^{18}F-NaF. Physiologic uptake and benign and indeterminate lesions were then removed by the readers so that only highly suggestive foci were included in the analysis. In these men, exact lesion number was impossible to count, thus only the TB and the TLU were recorded.

Lesion detection rates and imaging concordance were determined at the patient level and lesion level for the 3 agents. Positive lesions in the same location on different scans were considered concordant regardless of variation in volume or extent. Lesion detection rate and imaging concordance were correlated with PSA, castration status, and treatment at the time of imaging. Men were considered castration-resistant (CRPC) if they had a history of androgen deprivation therapy (ADT) with castrate serum testosterone (<50 ng/dL) plus biochemical or radiologic progression, and were considered castration-sensitive (CSPC) if they never had ADT or if they had a history of ADT but did not fit criteria of CRPC.

Statistical Analysis

^{18}F-DCFPyL, ^{18}F-NaF, and ^{18}F-FDG PET characteristics (number of lesions, TB, and TLU) were correlated to PSA values using Spearman rank correlation. Differences in imaging PET parameters across individual characteristics, such as castration status and treatment at the time of imaging, were evaluated using the Wilcoxon rank-sum test. Comparisons of number of lesions and TB between ^{18}F-NaF and ^{18}F-DCFPyL (for bone lesions only) and between ^{18}F-FDG and ^{18}F-DCFPyL were performed with the paired Wilcoxon test. Lesions were categorized as concordant or discordant across tracers. Concordance between tracers at the patient level was evaluated using Wilcoxon rank-sum and Spearman rank correlation. All tests were 2-sided, and P values < 0.05 were considered significant.

RESULTS

Population

Overall, a total of 67 patients (median age, 67.8 y; age range, 51–84 y) with documented metastatic PCa met criteria for the protocol between June 2017 and February 2020. Six patients were excluded from the analysis because there was no disease uptake on any of the PET/CT scans; therefore only 61 evaluable patients were analyzed. Seven patients (11.5%) had newly diagnosed metastatic PCa and had not received any treatment at the time of imaging. Further specific patient demographics are listed in Table 1. The mean time between ^{18}F-DCFPyL and ^{18}F-NaF and between ^{18}F-DCFPyL and ^{18}F-FDG scans was 7 d (range, 1–35 d) and 8 d (range, 1–33 d),

TABLE 1
Patient Demographics (n = 61)

Characteristic	Data
Median age (y)	67.8 (range, 51–84)
ISUP grade	
1	5 (8.2%)
2	6 (9.8%)
3	9 (14.8%)
4	15 (24.6%)
5	25 (41.0%)
Not available	1 (1.6%)
Initial treatment	
None	7 (11.5%)
Surgery (prostatectomy +/− lymph node dissection)	28 (45.9%)
Definitive radiation therapy +/− ADT	12 (19.6%)
ADT	7 (11.5%)
ADT + chemotherapy	5 (8.2%)
Cryotherapy	2 (3.3%)
Castration status	
Castration-sensitive	41 (67.3%)
Castration-resistant	20 (32.7%)
Median PSA (ng/mL)	9.97 (range 0.02–7270.8)
Median PSA doubling time (months)	5.1 (range 0.7–81.7)
Median PSA velocity (ng/mL/y)	15.4 (range 0.1–5967.4)
Therapy at time of imaging	
No treatment	34 (55.7%)
ADT	18 (29.5%)
ADT + other	3 (4.9%)
Other (chemotherapy, immunotherapy, estradiol patch)	6 (9.8%)

ISUP = International Society of Urological Pathologists.

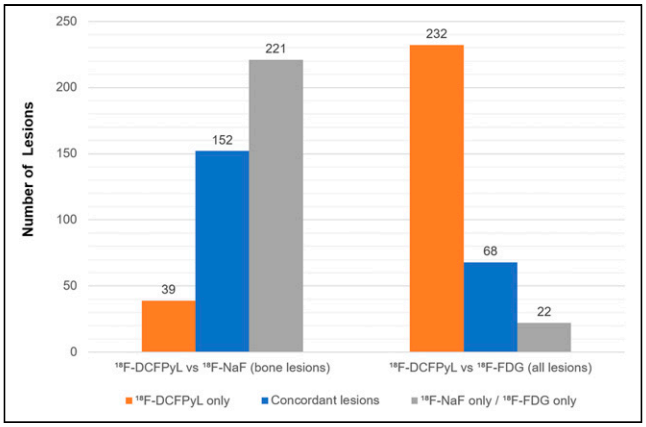

FIGURE 1. Lesion number comparisons.

respectively. Patients did not experience adverse events or clinically detected pharmacologic effects after PET scans.

Comparison Between ^{18}F-DCFPyL and ^{18}F-NaF (Group 1)

Patient-Based Detection Rate and Concordance Between Radiotracers. All 61 patients had at least 1 pathologic focus consistent with metastatic bone disease on ^{18}F-DCFPyL. The ^{18}F-NaF detection rate was 77.0% for metastatic bone disease.

The median percentage of bone lesions that were concordant between ^{18}F-DCFPyL and ^{18}F-NaF was 50%. The imaging concordance between ^{18}F-NaF and ^{18}F-DCFPyL was independent of castration status, PSA values, treatment at the time of imaging, and time from diagnosis to imaging.

Lesion-Based Detection Rate. A total of 412 bone lesions were detected by ^{18}F-DCFPyL or ^{18}F-NaF. Lesions from 6 patients with extensive disease ("superscans") were excluded from this analysis because an accurate lesion count was not feasible. ^{18}F-NaF detected 373 of 412 (90.5%) bone lesions and ^{18}F-DCFPyL detected 191 (46.4%). A total of 152 of these bone lesions were concordant between ^{18}F-NaF and ^{18}F-DCFPyL, 39 were detected by ^{18}F-DCFPyL only, and 221 were detected by ^{18}F-NaF only (Fig. 1). The median number of bone lesions detected by ^{18}F-NaF was higher than that by ^{18}F-DCFPyL ($P = 0.001$) (Fig. 2). Lesion tumor volume detected only by ^{18}F-NaF was significantly lower than that of lesions detected by both ^{18}F-NaF and ^{18}F-DCFPyL ($P < 0.05$). In this population, ^{18}F-DCFPyL identified 450 soft-tissue lesions (186 pelvic lymph nodes, 112 retroperitoneal lymph nodes, 92 distant lymph nodes, and 11 visceral lesions) in addition to the bone lesions.

Correlation with PSA. The number of lesions, TLU, and total TV derived from ^{18}F-DCFPyL and ^{18}F-NaF correlated with PSA and PSA velocity (Table 2). The strongest correlation was seen between PSA and TLU ($\rho = 0.6$, $P < 0.001$) and total TV ($\rho = 0.55$, $P < 0.001$) detected by ^{18}F-DCFPyL. These PET metrics showed a weak correlation with PSA doubling time.

The median number of bone lesions detected by ^{18}F-NaF was slightly higher than that by ^{18}F-DCFPyL at low PSA levels and rose with increasing PSA (Fig. 3A). The same trend was noted for TV, with a greater TV detected by ^{18}F-NaF than by ^{18}F-DCFPyL, but the difference was not significant.

Correlation with Treatment at the Time of Imaging. Men were subdivided into 2 groups according to their treatment at the time of imaging: 1 group consisted of 27 men receiving treatment (mainly ADT and chemotherapy) and the other group consisted of 34 men with no treatment at the time of imaging. Number of lesions, TB, and TLU were higher in the group receiving treatment than in men without treatment (P values ranging from 0.016 to 0.057) (Table 3).

For men without treatment, there was no significant difference in median number of bone lesions detected by ^{18}F-NaF versus ^{18}F-DCFPyL, but more bone lesions were detected by ^{18}F-NaF than by ^{18}F-DCFPyL among men receiving treatment (Fig. 3B). Although the difference was not significant, the same pattern was noted for TV with higher bone tumor volume detected by ^{18}F-NaF in comparison to ^{18}F-DCFPyL.

Correlation with Castration Status. Number of lesions, TB, and TLU showed a positive correlation with CRPC status (P values between 0.005 and 0.042) (Table 3).

In CSPC patients, there was no significant difference in median number of bone lesions detected by ^{18}F-NaF versus ^{18}F-DCFPyL, but more bone lesions were detected by ^{18}F-NaF among CRPC patients (9 vs. 5 lesions; $P = 0.014$) (Fig. 4A). The TB detected by ^{18}F-NaF was higher than that by ^{18}F-DCFPyL for CRPC patients ($P = 0.017$) and CSPC patients ($P = 0.051$).

Histopathology. A biopsy was performed in 32 patients (52.5%). Five patients had biopsies from 2 different locations. Among the 37 samples, 5 were prostate gland, 6 lymph nodes, 22 bone lesions, and 4 visceral lesions. Most of the samples (94.6%) demonstrated metastases of PCa. Of 22 bone lesions, ^{18}F-NaF demonstrated 2

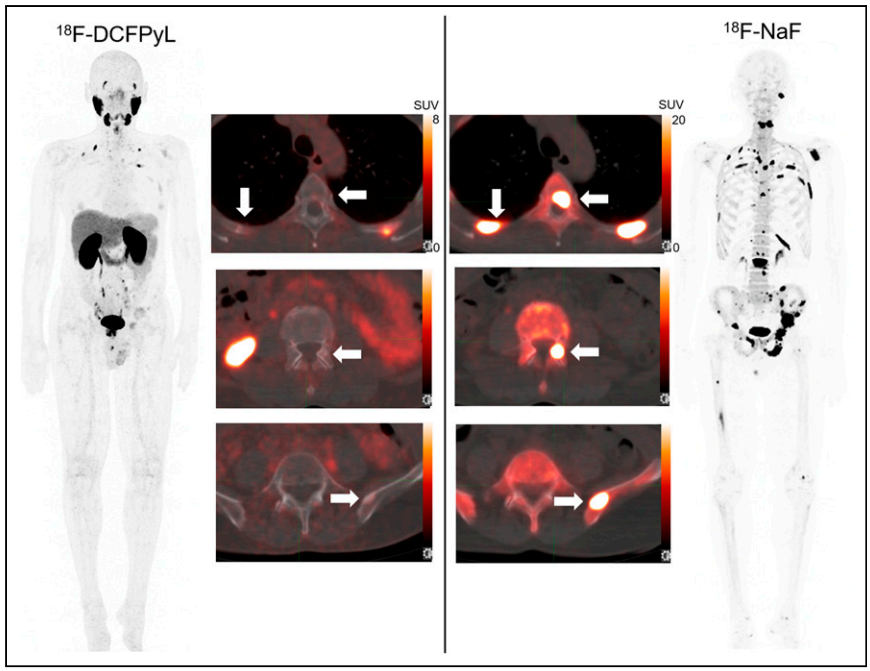

FIGURE 2. ^{18}F-DCFPyL (left) and ^{18}F-NaF (right) discordance. A 61-y-old man with metastatic PCa involving lymph nodes and bones. PSA at imaging was 49.69 ng/mL. More bone lesions were seen with ^{18}F-NaF than with ^{18}F-DCFPyL (arrows).

TABLE 2
Correlation of PSA Characteristics with PET Metrics Derived from ^{18}F-DCFPyL, ^{18}F-NaF, and ^{18}F-FDG, Using Spearman Correlation Coefficient

	^{18}F-DCFPyL		^{18}F-NaF		^{18}F-FDG	
Parameter	PSA	PSA velocity	PSA	PSA velocity	PSA	PSA velocity
No. of lesions	0.47 (<0.001)	0.38 (0.003)	0.41 (0.001)	0.25 (0.06)	0.21 (0.268)	0.39 (0.038)
Total lesion uptake	0.6 (<0.001)	0.53 (<0.001)	0.31 (0.014)	0.33 (0.015)	0.44 (0.014)	0.32 (0.087)
Total tumor burden	0.55 (<0.001)	0.5 (<0.001)	0.34 (0.007)	0.29 (0.028)	0.44 (0.016)	0.34 (0.074)

Expressed as correlation coefficient (ρ) with *P* values in parentheses.

false-positives (rib, sacrum) and 20 true-positives. ^{18}F-DCFPyL revealed 2 false-positives (rib, sacrum), 1 false-negative (sternum), and 34 true-positives (19 in bone).

Comparison Between ^{18}F-DCFPyL and ^{18}F-FDG (Group 2)

Patient-Based Detection Rate and Concordance Between Radiotracers. A cohort of 30 patients underwent both ^{18}F-DCFPyL and ^{18}F-FDG PET/CT imaging. The ^{18}F-FDG detection rate was 93.3% on a per-patient basis. The median percentage of lesions that were concordant between ^{18}F-DCFPyL and ^{18}F-FDG was 22% (Fig. 5). Imaging concordance between ^{18}F-DCFPyL and ^{18}F-FDG was higher in men with CRPC (66.5%) than CSPC (20%) (P = 0.019) and was independent of other factors.

Lesion-Based Detection Rate. Among the 322 lesions detected by ^{18}F-FDG or ^{18}F-DCFPyL (244 soft-tissue lesions and 78 bone lesions), 68 were concordant, 232 were detected by ^{18}F-DCFPyL only, and 22 were detected by ^{18}F-FDG only. The median number of lesions detected by ^{18}F-DCFPyL was 5 (interquartile range, 3–15.5), which was significantly higher than ^{18}F-FDG (median of 2 lesions [interquartile range, 1–3.5], P = 0.0003).

Correlation with PSA, Treatment at the Time of Imaging, and Castration Status. Most metrics derived from ^{18}F-FDG correlated with PSA and PSA velocity, castration status, and treatment at the time of imaging (Table 2; Fig. 3C).

^{18}F-DCFPyL demonstrated more lesions than ^{18}F-FDG regardless of PSA, treatment, and castration status (Fig. 4B).

The total TV detected by ^{18}F-DCFPyL was greater than that by ^{18}F-FDG in the group with a PSA > 10 ng/mL (P = 0.033), when patients were not on treatment (P = 0.044) and in the CSPC group (P = 0.017).

Histopathology. A biopsy was performed in 17 men who underwent ^{18}F-FDG, revealing 3 false-negatives (iliac, ischium, and prostate) and 15 true-positives for the PET tracer.

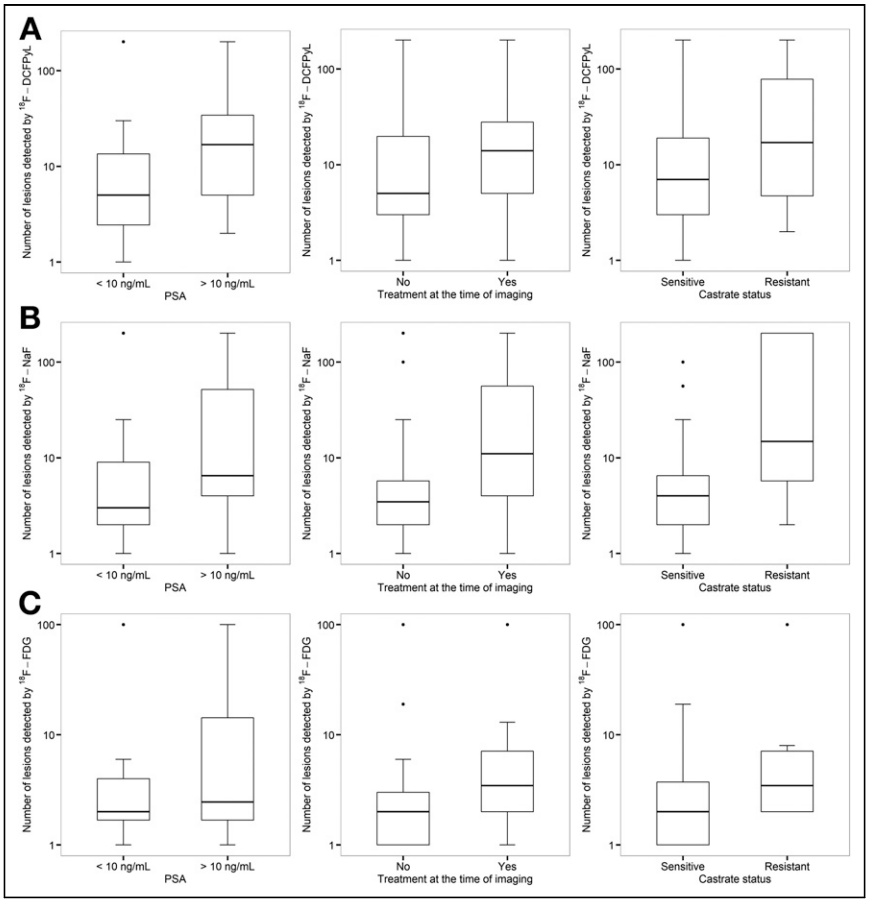

FIGURE 3. Number of lesions detected by ^{18}F-DCFPyL (A), ^{18}F-NaF (B), and ^{18}F-FDG (C) according to median PSA (left), treatment at the time of imaging (middle), and castration status (right).

DISCUSSION

Accurate assessment of disease burden is essential for the management of patients with metastatic PCa. However, it is unlikely that a single targeted imaging agent will detect all lesions given the heterogeneous nature of metastatic disease (*11*). With very different mechanisms of radiotracer uptake, the low percentage of concordant lesions among the 3 PET agents studied (^{18}F-DCFPyL, ^{18}F-NaF, and ^{18}F-FDG) supports the concept that many phenotypes of metastases exist, even within the same person.

In this study, ^{18}F-NaF showed the highest sensitivity for bone metastases. These results support the results in the study from Harmon et al. in which bone lesion detection rates for ^{18}F-NaF and a first-generation

TABLE 3
^{18}F-DCFPyL, ^{18}F-NaF, and ^{18}F-FDG Median Number of Lesions, Total Tumor Volume, and Total Lesion Uptake According to Median PSA, Treatment at the Time of Imaging, and Castration Status

	No. of lesions			Total tumor burden			Total lesion uptake		
Feature	Median	IQR	*P*	Median	IQR	*P*	Median	IQR	*P*
PSA (ng/mL)									
PyL			0.005			<0.001			<0.001
<10	5	2.5–13.5		12.7	4.3–34.2		99.9	26–232.2	
>10	17	5–34		62.8	14.8–200		680.9	154.1–3,211	
NaF			0.006			0.079			0.115
<10	2	0–4		6	0–41.1		49.6	0–1,373.4	
>10	5.5	2–34		13.4	3.4–252		130.8	41.4–3,736.4	
FDG			0.5			0.052			0.05
<10	2	1–4		6.2	2.4–23.9		28	7.8–58.5	
>10	2	1–13		48.8	3.8–191		211	18–941	
Treatment ongoing									
PyL			0.057			0.016			0.021
No	5	3–20		16.6	4.2–51.9		117	20.1–507.6	
Yes	14	5–28		36.4	13.4–174		305.3	138.4–1,487	
NaF			0.05			0.024			0.048
No	3	1–5		5.8	0.4–18.9		56.8	4.3–404.6	
Yes	6	1.5–30.5		54.6	1.2–190		1062	19.5–2,466.3	
FDG			0.04			0.036			0.032
No	1.5	1–3		5	0.7–25.1		18	5–59	
Yes	3.5	2–7		38.7	10–87.3		112.5	33.2–237.2	
Castration status									
PyL			0.042			0.013			0.018
CS	7	3–19		21.3	4.4–60.2		122.3	37.9–575.9	
CR	17	5–93		77	13.6–192		302.4	157.9–2,123	
NaF			0.012			0.005			0.012
CS	3	1–5		5.82	0.4–20.5		49.6	3–475.5	
CR	9	3–95		93.1	11.1–655		1,256.2	70.4–4,475.6	
FDG			0.057			0.153			0.108
CS	2	1–3		6.21	1.8–45.8		21	7–139	
CR	3.5	2–7		25.6	10–86.1		71.5	33.3–518.5	

Expressed as median, with interquartile ranges in parentheses and *P* values in italic.
IQR = interquartile range; PyL = ^{18}F-DCFPyL; NaF = ^{18}F-NaF; FDG = ^{18}F-FDG; CS = castration-sensitive; CR = castration-resistant

PSMA-targeting agent were 98.4% and 45.4%, respectively, which are similar to our detection rates (93% for ^{18}F-NaF vs. 46% for ^{18}F-DCFPyL) (*12*). Our findings also agree with the study by Uprimny et al. in which ^{18}F-NaF PET detected a higher number of metastatic bone lesions than ^{68}Ga-PSMA-11 PET (*13*). These results differ from 2 other studies that found no difference in diagnostic sensitivity for bone metastases between these 2 radiotracers (*14,15*).

It has been argued that ^{18}F-NaF scans are susceptible to false-positives due to benign disease mimicking metastases (*16*). However, in this series, in which histologic confirmation was available in several cases, there were only 2 false-positives among 22 osseous lesions detected with ^{18}F-NaF after trained nuclear medicine physicians eliminated obvious benign lesions from consideration. Because PCa cells induce bone formation in adjacent osteocytes, it is likely that only a few cancer cells can affect many regional osteocytes, leading to an amplification of signal on ^{18}F-NaF scans, heightening sensitivity compared with ^{18}F-DCFPyl. We believe that ^{18}F-NaF reflects active disease but may recognize disease below the detection threshold of ^{18}F-DCFPyL (*17,18*). The relatively high rates of recurrent disease after ^{177}Lu-PSMA therapy in sites not previously identified suggest there is a reservoir of PSMA-negative metastases in the bone that may be detectable by ^{18}F-NaF but not by PSMA radiotracers (*19*).

One explanation for the lesion mismatch between ^{18}F-NaF and ^{18}F-DCFPyl is that castration resistance could disproportionately

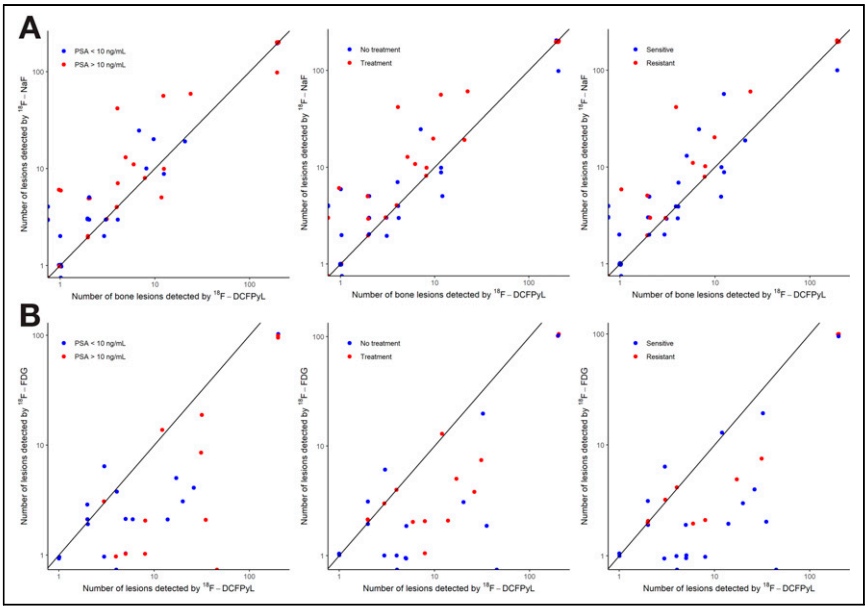

FIGURE 4. Comparison of median number of lesions detected by ^{18}F-NaF and ^{18}F-DCFPyL (bone lesions only) (A) and by ^{18}F-FDG and ^{18}F-DCFPyL (B) according to median PSA (left), treatment at the time of imaging (middle), and castration status.

influence the performance of ^{18}F-NaF relative to ^{18}F-DCFPyL (*20*). In CSPC patients, there was no difference in the median number of bone lesions detected by ^{18}F-NaF versus ^{18}F-DCFPyL, but more bone lesions were detected by ^{18}F-NaF among more heavily pretreated CRPC patients ($P = 0.014$). In immunohistochemistry studies, only 44% of bone metastases expressed PSMA, and osseous lesions with low PSMA detection were associated with CRPC, which could readily explain our findings of discordance with ^{18}F-NaF (*7*).

^{18}F-FDG– and PSMA-targeting agents showed low concordance in our study. PSMA-negative, FDG-positive lesions are thought to be more aggressive and are linked with poor outcomes as they are encountered more frequently in amphicrine and neuroendocrine phenotypes of CRPC (*21*). In our research, ^{18}F-DCFPyL detected significantly more lesions than ^{18}F-FDG ($P < 0.0001$) on both a per-patient and per-lesion basis regardless of castration or treatment status. In about 10% of men, some lesions were positive on ^{18}F-FDG and negative on ^{18}F-DCFPyL despite an overall higher lesion number seen by^{18}F-DCFPyL, implying that a limited number of metastases may exhibit aggressive metabolic features with low PSMA (FDG+, PSMA–) earlier in the course of disease (*22*). Indeed, similar to the study by Wang et al. (*23*), we noted discordance between the 2 scans with 22 of 322 lesions (6.8%) detected by ^{18}F-FDG alone in 8 of 30 patients (27%), of which 3 were CRPC and 5 were CSPC. These lesions may be clinically relevant, as decreased survival and therapeutic response have been noted in men with abnormal ^{18}F-FDG PET findings (*21*, *22,24,25*). ^{18}F-FDG uptake has been suggested as a biomarker for CRPC and when accompanied by negative ^{18}F-DCFPyL findings, may suggest evolution to neuroendocrine prostate cancer (*26*). Interestingly, as the disease progressed from CSPC to CRPC, concordance between ^{18}F-FDG and ^{18}F-DCFPyL scans increased ($P = 0.048$). The discordance among ^{18}F-DCFPyL, ^{18}F-FDG, and ^{18}F-NaF scans in individual lesions confirms phenotypic heterogeneity of PCa metastases, explaining, in part, the difficulty in eradicating such lesions.

The main limitation of this study was the lack of histologic proof for many of the suspected metastases. However, where biopsies were obtained, they overwhelmingly confirmed the presence of cancer in positive scans. Furthermore, readers had access to PET/CT images obtained with the other radiotracers, which may have biased the interpretation of faint uptake when scans were evaluated. However, these unmasked readings reflect daily practice. Finally, the metastatic population was broadly diverse and further investigation stratified by prior therapy may help clarify the respective roles of these radiotracers in the various states of PCa.

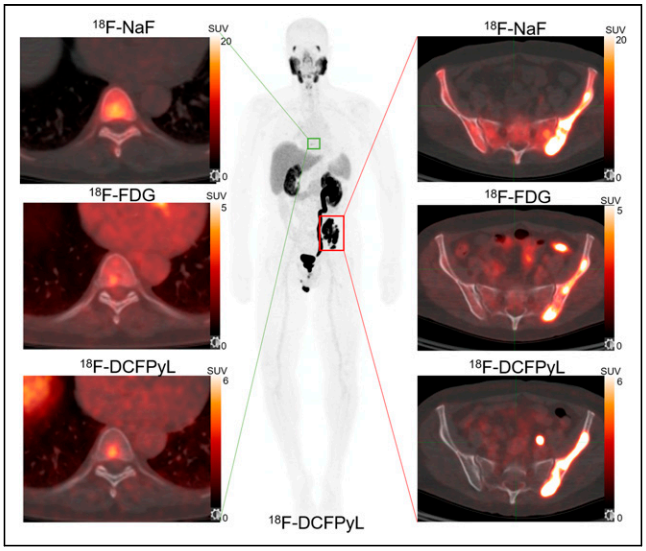

FIGURE 5. Concordant PET metastases. A 64-y-old man with metastatic CRPC. PSA at imaging was 464 ng/mL. Concordant pathologic foci were noted on all scans at T8 vertebral body and left iliac bone, consistent with metastasis.

CONCLUSION

Imaging men with metastatic PCa using ^{18}F-NaF, ^{18}F-DCFPyL, and ^{18}F-FDG PET demonstrated that ^{18}F-DCFPyL had the best overall performance, but concordance with other agents was low, reflecting phenotypic tumor differences. ^{18}F-NaF identified a significantly higher number of metastatic bone lesions than ^{18}F-DCFPyL. Our study suggests that ^{18}F-NaF might provide additional staging information compared with ^{18}F-DCFPyL, especially in castration-resistant patients and patients receiving treatment at the time of imaging. ^{18}F-DCFPyL functioned better than ^{18}F-FDG in overall lesion detection and was more concordant in CRPC. Further research is warranted to elucidate the utility of ^{18}F-FDG PET and ^{18}F-NaF as prognostic tools and complementary agents to ^{18}F-DCFPyL in understanding tumor heterogeneity patterns in PCa metastases.

DISCLOSURE

This project has been funded in whole or in part with federal funds from the National Cancer Institute, National Institutes of Health, under contract nos. 75N91019D00024, Task Order no. 75N91019F00129, and HHSN261200800001E. The content of this publication does not necessarily reflect the views of policies of the Department of Health and Human Services, nor does mention of trade names, commercial products, or organization imply endorsement by the US. Government. Aloÿse Fourquet is the recipient of a grant from the ARC Foundation for cancer research. No other potential conflict of interest relevant to this article was reported.

ACKNOWLEDGMENTS

We thank Anita Ton, Yolanda McKinney, Juanita Weaver, Philip Eclarinal, Alicia Forest, Chris Leyson, and Mona Cedo for their constant patient care. Thank you to the patients and their families for the sacrifices they made in contributing to this research.

KEY POINTS

QUESTION: How does ^{18}F-DCFPyL uptake compare with that of ^{18}F-NaF and ^{18}F-FDG PET/CT in men with metastatic PCa?

PERTINENT FINDINGS: In a prospective study of 67 men with metastatic PCa, ^{18}F-DCFPyL was the most versatile PET agent but ^{18}F-NaF detected more bone metastasis. Substantial tumor heterogeneity was revealed, with only 50% concordance between ^{18}F-DCFPyL and ^{18}F-NaF and 22% concordance between ^{18}F-DCFPyL and^{18}F-FDG.

IMPLICATIONS FOR PATIENT CARE: ^{118}F-FDG and ^{18}F-NaF could be complementary agents to ^{18}F-DCFPyL in staging and illustrating heterogeneous disease characteristics that could optimize treatment strategies for men with metastatic PCa.

REFERENCES

1. American Cancer Society. *Cancer Facts & Figures 2020.* American Cancer Society; 2020.
2. Jackson SE, Chester JD. Personalised cancer medicine. *Int J Cancer.* 2015;137:262–266.
3. Mateo J, Carreira S, Sandhu S, et al. DNA-repair defects and Olaparib in metastatic prostate cancer. *N Engl J Med.* 2015;373:1697–1708.
4. Langsteger W, Rezaee A, Pirich C, Beheshti M. ^{18}F-NaF-PET/CT and ^{99m}Tc-MDP bone scintigraphy in the detection of bone metastases in prostate cancer. *Semin Nucl Med.* 2016;46:491–501.
5. Löfgren J, Mortensen J, Rasmussen SH, et al. A prospective study comparing ^{99m}Tc-hydroxyethylene-diphosphonate planar bone scintigraphy and whole-body SPECT/CT with ^{18}F-fluoride PET/CT and ^{18}F-fluoride PET/MRI for diagnosing bone metastases. *J Nucl Med.* 2017;58:1778–1785.
6. Ghosh A, Heston WDW. Tumor target prostate specific membrane antigen (PSMA) and its regulation in prostate cancer. *J Cell Biochem.* 2004;91:528–539.
7. Silver DA, Pellicer I, Fair WR, Heston WD, Cordon-Cardo C. Prostate-specific membrane antigen expression in normal and malignant human tissues. *Clin Cancer Res.* 1997;3:81–85.
8. Wright GL, Haley C, Beckett ML, Schellhammer PF. Expression of prostate-specific membrane antigen in normal, benign, and malignant prostate tissues. *Urol Oncol.* 1995;1:18–28.
9. Reinicke K, Sotomayor P, Cisterna P, Delgado C, Nualart F, Godoy A. Cellular distribution of Glut-1 and Glut-5 in benign and malignant human prostate tissue. *J Cell Biochem.* 2012;113:553–562.
10. Jadvar H, Desai B, Ji L, et al. Baseline ^{18}F-FDG PET/CT parameters as imaging biomarkers of overall survival in castrate-resistant metastatic prostate cancer. *J Nucl Med.* 2013;54:1195–1201.
11. Tolkach Y, Kristiansen G. The heterogeneity of prostate cancer: a practical approach. *Pathobiology.* 2018;85:108–116.
12. Harmon SA, Bergvall E, Mena E, et al. A prospective comparison of ^{18}F-sodium fluoride PET/CT and PSMA-targeted ^{18}F-DCFBC PET/CT in metastatic prostate cancer. *J Nucl Med.* 2018;59:1665–1671.
13. Uprimny C, Svirydenka A, Fritz J, et al. Comparison of [^{68}Ga]Ga-PSMA-11 PET/CT with [^{18}F]NaF PET/CT in the evaluation of bone metastases in metastatic prostate cancer patients prior to radionuclide therapy. *Eur J Nucl Med Mol Imaging.* 2018;45:1873–1883.
14. Rowe SP, Li X, Trock BJ, et al. Prospective comparison of PET imaging with PSMA-targeted ^{18}F-DCFPyL versus Na18F for bone lesion detection in patients with metastatic prostate cancer. *J Nucl Med.* 2020;61:183–188.
15. Zhou J, Gou Z, Wu R, Yuan Y, Yu G, Zhao Y. Comparison of PSMA-PET/CT, choline-PET/CT, NaF-PET/CT, MRI, and bone scintigraphy in the diagnosis of bone metastases in patients with prostate cancer: a systematic review and meta-analysis. *Skeletal Radiol.* 2019;48:1915–1924.
16. Usmani S, Ahmed N, Muzaffar S, et al. Spectrum of false positive ^{18}F-sodium fluoride (NaF) bone PET/CT findings in oncology imaging: a narrative pictorial review of cases from a single institution. *Hell J Nucl Med.* 2020;23:67–75.
17. Rodrigues G, Bae K, Roach M, et al. Impact of ultrahigh baseline PSA levels on biochemical and clinical outcomes in two radiation therapy oncology group prostate clinical trials. *Int J Radiat Oncol Biol Phys.* 2011;80:445–452.
18. Koo KC, Park SU, Kim KH, et al. Predictors of survival in prostate cancer patients with bone metastasis and extremely high prostate-specific antigen levels. *Prostate Int.* 2015;3:10–15.
19. Violet J, Sandhu S, Iravani A, et al. Long-term follow-up and outcomes of retreatment in an expanded 50-patient single-center phase II prospective trial of ^{177}Lu-PSMA-617 theranostics in metastatic castration-resistant prostate cancer. *J Nucl Med.* 2020;61:857–865.
20. Afshar-Oromieh A, Debus N, Uhrig M, et al. Impact of long-term androgen deprivation therapy on PSMA ligand PET/CT in patients with castration-sensitive prostate cancer. *Eur J Nucl Med Mol Imaging.* 2018;45:2045–2054.
21. Hofman MS, Violet J, Hicks RJ, et al. [^{177}Lu]-PSMA-617 radionuclide treatment in patients with metastatic castration-resistant prostate cancer (LuPSMA trial): a single-centre, single-arm, phase 2 study. *Lancet Oncol.* 2018;19:825–833.
22. Jadvar H. Is there utility for FDG PET in prostate cancer? *Semin Nucl Med.* 2016;46:502–506.
23. Wang B, Liu C, Wei Y, et al. A prospective trial of ^{68} Ga-PSMA and ^{18} F-FDG PET/CT in nonmetastatic prostate cancer patients with an early PSA progression during castration. *Clin Cancer Res.* 2020;26:4551–4558.
24. Meirelles GSP, Schoder H, Ravizzini GC, et al. Prognostic value of baseline [^{18}F] fluorodeoxyglucose positron emission tomography and ^{99m}Tc-MDP bone scan in progressing metastatic prostate cancer. *Clin Cancer Res.* 2010;16:6093–6099.
25. Zukotynski KA, Kim CK, Gerbaudo VH, et al. ^{18}F-FDG-PET/CT and ^{18}F-NaF-PET/CT in men with castrate-resistant prostate cancer. *Am J Nucl Med Mol Imaging.* 2014;5:72–82.
26. Jadvar H, Velez EM, Desai B, Ji L, Colletti PM, Quinn DI. Prediction of time to hormonal treatment failure in metastatic castration-sensitive prostate cancer with ^{18}F-FDG PET/CT. *J Nucl Med.* 2019;60:1524–1530.